6-26-2014

Rapid reservoir erosion, hyperconcentrated flow, and downstream deposition triggered by breaching of 38 m tall Condit Dam, White Salmon River, Washington

Andrew C. Wilcox
University of Montana - Missoula, andrew.wilcox@umontana.edu

Jim E. O'Connor
U.S. Geological Survey - Oregon Water Science Center

Jon J. Major
U.S. Geological Survey - Cascades Volcano Observatory

Recommended Citation

Wilcox, A. C., J. E. O'Connor, and J. J. Major (2014), Rapid reservoir erosion, hyperconcentrated flow, and downstream deposition triggered by breaching of 38 m tall Condit Dam, White Salmon River, Washington, J. Geophys. Res. Earth Surf., 119, 1376–1394, doi:10.1002/2013JF003073.

AGU PUBLICATIONS

JGR

Journal of Geophysical Research: Earth Surface

RESEARCH ARTICLE
10.1002/2013JF003073

Key Points:
- The October 2011 breaching of Condit Dam produced dramatic geomorphic responses
- Breaching triggered landsliding and rapid evacuation of reservoir sediments
- Sediment initially moved downstream in hyperconcentrated flow and draped the bed

Supporting Information:
- Readme
- Figure S1–S7
- Animation S1
- Animation S2
- Animation S3
- Animation S4
- Animation S5
- Table S1
- Table S2

Correspondence to:
A. C. Wilcox,
andrew.wilcox@umontana.edu

Citation:
Wilcox, A. C., J. E. O'Connor, and J. J. Major (2014), Rapid reservoir erosion, hyperconcentrated flow, and downstream deposition triggered by breaching of 38 m tall Condit Dam, White Salmon River, Washington, *J. Geophys. Res. Earth Surf.*, *119*, 1376–1394, doi:10.1002/2013JF003073.

Received 21 DEC 2013
Accepted 30 APR 2014
Accepted article online 5 MAY 2014
Published online 26 JUN 2014

Rapid reservoir erosion, hyperconcentrated flow, and downstream deposition triggered by breaching of 38 m tall Condit Dam, White Salmon River, Washington

Andrew C. Wilcox[1], Jim E. O'Connor[2], and Jon J. Major[3]

[1]Department of Geosciences, University of Montana, Missoula, Montana, USA, [2]Oregon Water Science Center, U.S. Geological Survey, Portland, Oregon, USA, [3]Cascades Volcano Observatory, U.S. Geological Survey, Vancouver, Washington, USA

Abstract Condit Dam on the White Salmon River, Washington, a 38 m high dam impounding a large volume (1.8 million m^3) of fine-grained sediment (60% sand, 35% silt and clay, and 5% gravel), was rapidly breached in October 2011. This unique dam decommissioning produced dramatic upstream and downstream geomorphic responses in the hours and weeks following breaching. Blasting a 5 m wide hole into the base of the dam resulted in rapid reservoir drawdown, abruptly releasing ~1.6 million m^3 of reservoir water, exposing reservoir sediment to erosion, and triggering mass failures of the thickly accumulated reservoir sediment. Within 90 min of breaching, the reservoir's water and ~10% of its sediment had evacuated. At a gauging station 2.3 km downstream, flow increased briefly by 400 $m^3 s^{-1}$ during passage of the initial pulse of released reservoir water, followed by a highly concentrated flow phase—up to 32% sediment by volume—as landslide-generated slurries from the reservoir moved downstream. This hyperconcentrated flow, analogous to those following volcanic eruptions or large landslides, draped the downstream river with predominantly fine sand. During the ensuing weeks, suspended-sediment concentration declined and sand and gravel bed load derived from continued reservoir erosion aggraded the channel by >1 m at the gauging station, after which the river incised back to near its initial elevation at this site. Within 15 weeks after breaching, over 1 million m^3 of suspended load is estimated to have passed the gauging station, consistent with estimates that >60% of the reservoir's sediment had eroded. This dam removal highlights the influence of interactions among reservoir erosion processes, sediment composition, and style of decommissioning on rate of reservoir erosion and consequent downstream behavior of released sediment.

1. Introduction

The October 2011 breach of Condit Dam on the White Salmon River, Washington, was one of several large dams removed in recent years in a growing movement of river restoration. Within the U.S., over 1000 dams have been decommissioned since 1912 [*American Rivers*, 2013] to address economic, environmental, safety, and regulatory concerns [*Graf*, 2002]. Nearly all have been of small dams less than 10 m high on low-gradient rivers, many with modest physical consequences but nevertheless highly visible [*Doyle et al*., 2003a, 2003b; *Wildman and MacBroom*, 2005; *Pearson et al*., 2011; *Sawaske and Freyberg*, 2012; *Collins et al*., 2013; *DeGraff and Evans*, 2013]. Dam removals, particularly of large dams such as Condit that impound voluminous sediment, create opportunities to understand the processes by which rivers reconnect after several decades of interrupted movement of water, sediment, and aquatic life [*Service*, 2011].

Studies of the consequences of dam removal show that geomorphic responses are site specific in some respects but also share several controlling factors across a range of rivers, dams, and removal methods. Reservoir erosion and channel evolution upstream of breached dams are influenced by dam height and resulting base-level fall for the upstream river; rate and style of dam removal; volume, grain size, distribution, and management of reservoir sediment; reservoir geometry; and post-breach river flows [*Pizzuto*, 2002; *Wildman and MacBroom*, 2005; *Downs et al*., 2009; *Pearson et al*., 2011; *Cannatelli and Curran*, 2012; *Major et al*., 2012; *Sawaske and Freyberg*, 2012]. Downstream consequences are controlled partly by reservoir erosion dynamics but also depend on sediment characteristics, channel and valley slope, confinement, bed forms, and distance to downstream receiving features such as larger rivers, lakes, and oceans [*Doyle et al*., 2003a; *Kibler et al*., 2011; *Pearson et al*., 2011; *Major et al*., 2012; *Draut and Ritchie*, 2013]. Process controls may evolve

Table 1. Dam Height, Stored Sediment Volume, and Sediment Composition of Recent Dam Removals and Failures

Year of Removal	River	Dam	Dam Height (m)	Stored Sediment Volume (m^3)	Sediment Composition	Source
2007	Calapooia, OR	Brownsville	2–3	14,000	gravel	*Walter and Tullos* [2010]
2007	Sandy, OR	Marmot	15	750,000	~50% gravel, 50% sand	*Major et al.* [2012]
2007	Dahan, Taiwan	Barlin[a]	38	10.5 million	gravel, sand	*Tullos and Wang* [2014]
2008	Clark Fork, MT	Milltown	13	5.5 million[b]	sand, gravel	*USEPA* [2004] and *Evans and Wilcox* [2013]
2009	Rogue, OR	Savage Rapids	12	150,000	70% sand, 30% gravel	*Bountry et al.* [2013]
2009	Wind, WA	Hemlock	8	55,000[c]	~80% sand, 10% gravel, 10% silt & clay	*Randle and Greimann* [2004] and *Magirl et al.* [2010]
2011	White Salmon, WA	Condit	38	1.8 million	60% sand, 35% silt & clay, 5% gravel	*Kleinfelder* [2007] and *Mead and Hunt et al.* [2011]
2011–2012	Elwha, WA	Elwha	32	4.6 ± 1.5 million	70% silt and clay, 25% sand, 5% gravel	*Czuba et al.* [2011a] and *Draut and Ritchie* [2013]
2011–2014	Elwha, WA	Glines Canyon	64	21.6 ± 3 million	50% silt & clay, 35% sand, 15% gravel	

[a]Barlin Dam failed in 2007 as a result of a typhoon. Although not an intentional removal, its dam and reservoir properties and postfailure geomorphic response provide a relevant point of comparison for recent dam removals.
[b]Approximately 40% of this sediment was mechanically excavated as part of Superfund remediation efforts.
[c]Actual volume of material mechanically removed from the reservoir, in contrast to the 42,000 m^3 of sediment estimated to be in storage prior to breaching (B. Coffin, U.S. Forest Service, written communication, 2013).

temporally and with upstream and downstream changes. For example, the rate of reservoir sediment erosion may initially depend on base-level change and the style of erosion but later depend more strongly on flow conditions [*Pearson et al.*, 2011; *Cannatelli and Curran*, 2012; *Major et al.*, 2012].

The Condit Dam removal is an end-member combination for several of these controlling factors. The dam was tall at 38 m; at the time of its removal, Condit was the tallest U.S. dam intentionally removed, although this mantle has now been assumed by removal of the 64 m high Glines Canyon Dam on the Elwha River, Washington. The 1.8 million m^3 of reservoir sediment impounded at Condit was exceeded among intentional dam removals only by the 5.5 million m^3 at Milltown Dam, Montana (40% of which was excavated prior to removal as part of Superfund remediation [*Wilcox*, 2010]), and the 21–26 million m^3 impounded by the two Elwha River dams [*Duda et al.*, 2011; *Warrick et al.*, 2012; *Draut and Ritchie*, 2013] (Table 1). In comparison to recent removals of tall dams on rivers draining mountainous areas, the accumulated sediment at Condit, which consisted of mostly sand, silt, and clay, was distinctly finer (Table 1), with the exception of the similarly fine-grained reservoir sediment behind the Elwha River dams [*Czuba et al.*, 2011a; *Draut and Ritchie*, 2013]. Condit Dam was abruptly breached and the reservoir was rapidly emptied, in contrast to other removals of large dams impounding fine sediment. For example, the Elwha River dam removals [*Warrick et al.*, 2012; *Draut and Ritchie*, 2013] and the Milltown Dam removal [*Evans and Wilcox*, 2013] were staged, multiyear processes. Other tall dams that have been breached abruptly contained mostly coarse sediment, such as Marmot Dam, Oregon [*Major et al.*, 2012]; Savage Rapids Dam, Oregon [*Bountry et al.*, 2013]; and Barlin Dam, Taiwan, which failed during a 2007 typhoon [*Tullos and Wang*, 2014]. The Condit removal therefore provides a unique case study of dam removal, one in which the consequences were particularly substantial and rapid. Moreover, it provides a guide to the range of possible processes and outcomes as dam removals continue as a means of river restoration.

Here we present an analysis of reservoir evacuation and the coupled downstream transport of sediment to document key geomorphic processes and rates. Our analysis relies on measurements of water and sediment evacuation from the reservoir and of downstream flow and sediment transport. We focus on two time periods: (1) the 5 h of initial evacuation of water and sediment from the reservoir on the afternoon of breaching (26 October 2011) and (2) the 15 weeks of continued reservoir erosion, sediment transport, and channel

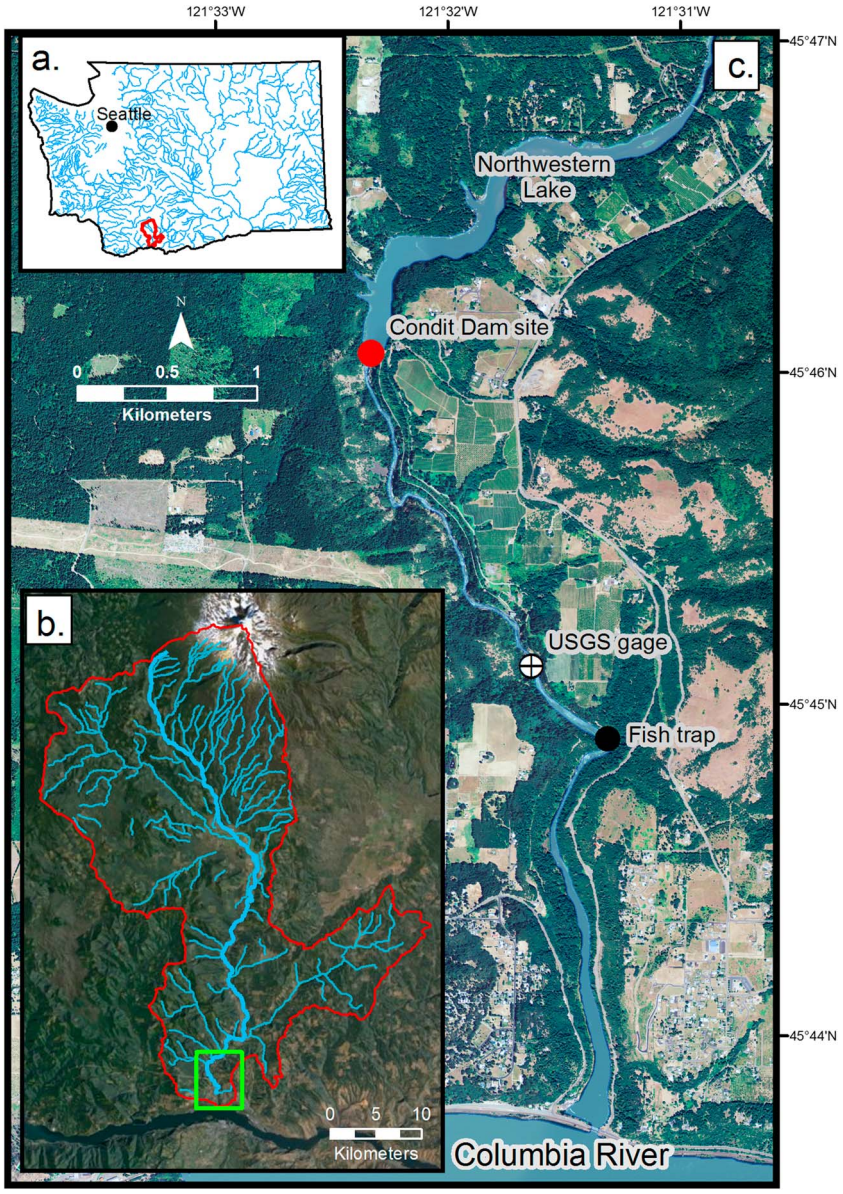

Figure 1. White Salmon River study area, showing (a) location of White Salmon watershed in state of Washington; (b) aerial map of watershed with area influenced by dam removal in green box; and (c) lower White Salmon River from Northwestern Lake to Columbia River confluence, including Condit Dam site and two sites where downstream measurements were taken: USGS White Salmon River near Underwood gauge, and White Salmon fish trap facility (map courtesy of E. Colaiacomo).

evolution subsequent to breaching (27 October 2011 to 4 February 2012). We show that rapid drawdown of a reservoir containing thickly accumulated fine-grained sediment caused instability and landslides within the reservoir sediment. Those mass failures rapidly mobilized a substantial portion of the impounded sediment, resulting in hyperconcentrated streamflow having sediment concentrations exceeding 30% by volume. Time-lapse videos of reservoir drainage and downstream passage of the water and sediment pulse are provided in the supporting information. Draping of the channel corridor with sand by muddy hyperconcentrated flow was followed by days of channel aggradation, and subsequent incision, as sand and gravel bed material moved downstream. Our observations and measurements document a unique mode of reservoir erosion and downstream sediment transport relative to previous dam removals, yet one that may be relevant to future large dam removals and to other processes, such as landslides, volcanic eruptions, and natural dam failures that rapidly load rivers with sediment.

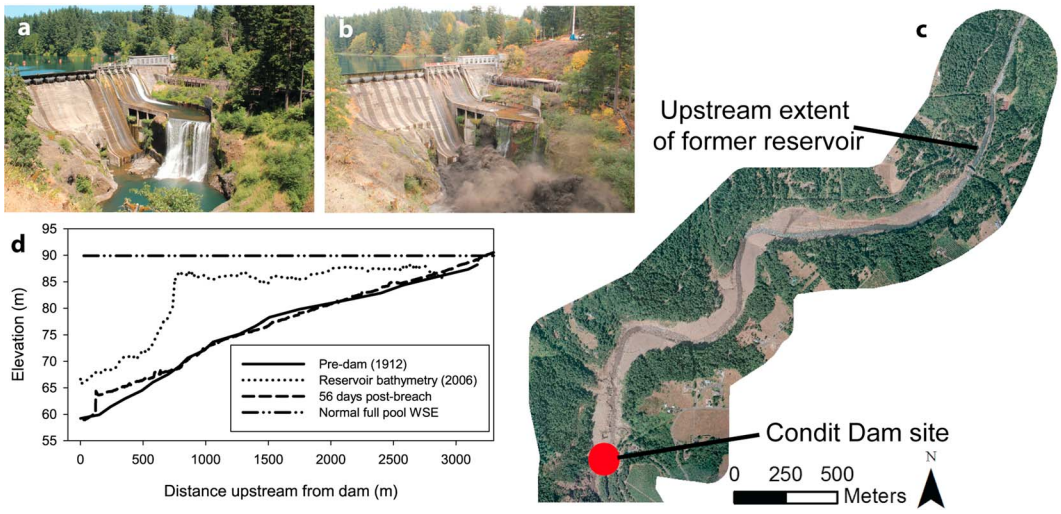

Figure 2. Condit Dam and reservoir: (a) Condit Dam before breaching (August 2011); (b) Condit Dam immediately following breaching, showing initial emergence of reservoir water and sediment from blast hole at base of dam (26 October 2011) (S. Stampfli and A. Maser photos); (c) post-breach aerial photograph of reach of White Salmon River formerly impounded by Condit Dam; and (d) longitudinal profiles of White Salmon River through area impounded by Condit Dam, including pre-dam (1912; digitized from pre-dam contours and smoothed), 2006 (showing reservoir sediment accumulation), and post-breach (coffer dam evident near downstream end of profile); normal full pool water surface elevation of reservoir is also shown.

2. Condit Dam and the White Salmon River

Condit Dam was a 14.7 MW hydroelectric facility constructed in 1912–1913 on the White Salmon River, 5.3 km upstream from the Columbia River (Figures 1 and 2) . The dam was breached in late 2011 and removed in 2012 as the lowest-cost alternative for providing fish passage, as would have been required to renew the facility's operating license [*Federal Energy Regulatory Commission*, 2002].

Northwestern Lake, the reservoir impounded by Condit Dam, extended 2.9 km upstream, covering 37 ha with 1.6 million m^3 of water at a normal pool elevation of 89.9 m [*Mead and Hunt et al*., 2011]. Over its nearly 100 year existence, the reservoir trapped 1.8 million m^3 of sediment [*Finley Engineering*, 2006]. This sediment came from an upstream contributing area of 990 km^2 in the southern Washington Cascade Range, including the southwestern flank of Mount Adams stratovolcano. Sediment yield inferred from reservoir sediment accumulation, ~30 tonnes $km^{-2}\,yr^{-1}$ (assuming a bulk sediment density of 1.5 tonnes m^{-3}), is modest but within the range of typical sediment yields of the Cascade Range [e.g., *Ambers*, 2001; *Roering et al*., 2010; *Czuba et al*., 2011b]. The reservoir sediment was 60% sand, 35% silt and clay, and 5% gravel (percentages estimated from sediment cores and rounded from values reported in *G&G Associates* [2004], *Kleinfelder* [2007], and *Mead and Hunt et al*. [2011]). Most sediment was deposited in a delta that extended more than 2 km downstream from the head of the reservoir and was more than 18 m thick locally (Figure 2d).

Near the dam site, the White Salmon River flows through a narrow bedrock valley. The pre-dam average channel slope through the reservoir reach is about 0.009 m/m (Figure 2d). Bedrock confinement extends upstream for several kilometers, including the 3 m tall Husum Falls 7 km upstream of the dam site. Downstream of the dam site, the river flows 3.7 km through a confined bedrock gorge, with a channel slope of 0.01 m/m, and then 1.6 km farther within an expanding valley where the water level is influenced by the backwater pool behind Bonneville Dam on the Columbia River (Figure 1).

Decommissioning of Condit Dam was uniquely rapid for a tall dam impounding substantial fine-grained sediment. To facilitate swift emptying of the reservoir, a tunnel was drilled partly through the 24 m wide base of the dam, followed by breach-day blasting of an approximately 5 m diameter hole through the remaining concrete plug. Detonation was at 12:08 on 26 October 2011, resulting in rapid drainage of the reservoir pool and sediment evacuation (Figures 2b, 3, and S1 and Animation S1). The rest of the dam structure was removed over the following year.

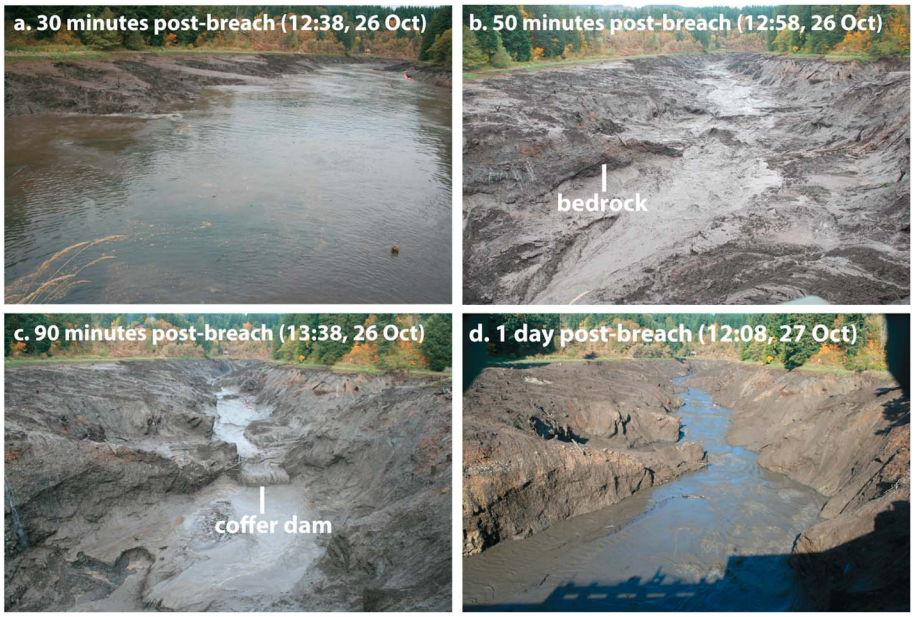

Figure 3. Time series of reservoir drainage; images taken from dam crest facing upstream show lower ~600 m of former Northwestern Lake. (a) Reservoir water-surface elevation has declined by 10 m, and slump scars indicate onset of landslides; (b) mass failures, exposed bedrock, and slurry in channel; (c) mass failures have slowed, and incision has exposed coffer dam; an estimated 160,000 m^3 of erosion has occurred in the visible reach as of this time; and (d) side slopes show little change relative to Figure 3c, eroded material from farther upstream in transport. Videos of time-lapse imagery from this camera station are provided in the supporting information.

3. Monitoring the Response to Dam Breaching

At the reservoir and downstream, we monitored the breaching and subsequent geomorphic response. Our primary efforts focused on measurements during the day of the breach, but continued monitoring and measurements documented geomorphic conditions during the following several weeks.

3.1. Reservoir Erosion

At the reservoir, we combined photographic methods and bathymetric and lidar surveys to document reservoir drawdown and the consequent spatial and temporal rates, magnitudes, and processes of erosion. Direct measurements were not possible because of limited access to what was a dynamic and unstable environment.

Multiple cameras located around the reservoir and aerial video recorded reservoir drawdown and initial erosion. Three time-lapse cameras (see *Major et al.* [2010] for specifications) mounted on Condit Dam and oriented upstream recorded one to four images per minute, documenting drawdown and erosion in a straight 650 m reach from the dam to the first river bend upstream (Figure 2c). Erosion in this reach was also recorded by a camera positioned on the right bank 650 m upstream of the dam and pointed downstream (20 images per minute on breach day; courtesy of A. Maser and S. Stampfli). A camera positioned on the right bank 750 m upstream from the dam, and facing across the reservoir, extended the area within camera range. This camera was in place until the day after breaching (Animation S2) and recorded four images per hour (courtesy of D. Gathard). Aerial video of the lower 800 m of the reservoir during the afternoon of breaching (courtesy of PacifiCorp) augmented the time-lapse images. We do not have breach-day time-lapse imagery for reaches of the reservoir farther upstream but instead rely on ground photos from several observers.

Time-lapse photography was also used to estimate reservoir erosion in the ensuing weeks. The cameras on the dam recorded the lower 650 m of reservoir at intervals of one to six images per hour from the day after breaching through mid-January 2012. Another camera, positioned 650 m upstream of the dam and directed upstream, recorded one image per minute from 16:19 on breach day through 9 November 2011 (courtesy of D. Gathard). A camera 1.3 km upstream of the dam, directed upstream, recorded continued erosion from a 700 m long reach extending to 2 km upstream between 27 October and 14 December 2011 (e.g., Animation S3). We also gathered additional time-stamped, georeferenced photos from other locations in the upper reservoir.

To determine the total sediment volume eroded from the reservoir in the first 8 weeks (56 days) after breaching, a digital elevation model (DEM) generated from an airborne lidar survey conducted on 21 December 2011 was differenced from a DEM of pre-breach topography [*Riverbend Engineering and JR Merit*, 2012]. The DEM of pre-breach reservoir topography was derived from a 2006 bathymetry survey of the reservoir, in which transects were measured at 15 m intervals from the dam to 2700 m upstream, near the upstream end of the reservoir [*Finley Engineering*, 2006]. The post-breach lidar survey extended to 3000 m upstream of the dam [*Watershed Sciences Inc.*, 2012].

To develop estimates of the temporal trajectory of reservoir erosion between the 26 October breaching and 21 December lidar survey, we combined the time-lapse photography, high-resolution (0.2 m pixel) color aerial orthophotographs taken 1 week after breaching (2 November) [*Riverbend Engineering and JR Merit*, 2012], and the two DEMs (2006 pre-breach bathymetry and 21 December 2011 lidar). By overlaying all these resources, we were able to define polygons on the DEMs that represent sub-reaches of the reservoir visible in the time-lapse photographs. From the time-lapse and other photographs, we identified the times when erosion visibly started and ended in each sub-reach polygon. To determine volumes of erosion in each of the defined sub-reaches, we conducted volumetric-change analyses by subtracting the post-breach DEM from the pre-breach DEM within each defined polygon using Quick Terrain Modeler software. Because we know when erosion started and stopped within each polygon, we are able to partition the total erosion up to the 21 December 2011 lidar survey to specific areas of the reservoir and to specific time intervals.

Our method for estimating reservoir erosion has several sources of uncertainty. The analysis area was confined to extent of the 2006 bathymetric survey, which is subject to elevation uncertainties as a result of the data collection and DEM construction methods employed. Erosion outside the area of the 2006 survey, in small tributary channels and in the 300 m upstream of the reservoir extent (between 2700 and 3000 m upstream), is not included in our calculations. Because the pre-breach DEM was constructed from 2006 data, additional sediment accumulation in the 5 years between the 2006 survey and breaching is not accounted for, although this error is likely small because the estimated average annual sediment flux (~20,000 $m^3\,yr^{-1}$) is modest. Additionally, the 21 December 2011 post-breach lidar does not account for the volume of material under the low-flow (21.5 $m^3\,s^{-1}$) river surface within the reservoir reach at the time of the survey. Our method of estimating the temporal sequence of erosion within different sub-reaches is also constrained by camera coverage and other uncertainties. We judge that collectively these factors result in an underestimate of the reservoir-erosion values calculated for each specific time period.

3.2. Downstream Response

Monitoring of the downstream sedimentologic response to breaching relied primarily on measurements of stage and suspended sediment at a USGS gauging station 2.3 km downstream of the dam site (Figure 1; White Salmon River near Underwood, station 14123500). At this site, continuous recording of flow stage (at 15 min intervals) is part of normal gauge operations; stage is related to discharge on the basis of measured stage-discharge ratings. Suspended sediment in flow past the gauge was sampled 126 times between 21 October 2011 and 4 February 2012, including 35 samples over a 4 h period starting shortly after the breach. The measurements were made by a combination of pump sampler, depth-integrated sampling from a cableway, and hand-dip sampling. Of the suspended-sediment samples at the gauge, most (89) were by automated pump sampler. Stage and sediment measurements at the gauge were supplemented by video, repeat photography, and sedimentologic analyses of deposits emplaced during and after breaching. All suspended-sediment and deposit samples were analyzed for concentration and grain size at the USGS Cascades Volcano Observatory sediment laboratory. Owing to changing channel geometry, the USGS made nine post-breach discharge measurements between 27 October 2011 (the day after breaching) and 4 February 2012. Six of those measurements were considered sufficiently reliable to publish and define post-breach stage-discharge relations (http://waterdata.usgs.gov/nwis/measurements/?site_no=14123500).

Supplemental sediment-concentration measurements were acquired using the same techniques at the White Salmon fish trap facility, 0.7 km downstream from the gauge (3.0 km downstream from the dam). These included eight suspended-sediment samples during breach day, eight samples the day following, and two samples 5 days after breaching.

Computed suspended-sediment flux is the product of sediment concentration (in mg L^{-1}) and discharge ($m^3 s^{-1}$) [*Gray and Simoes*, 2008] and reported in tonnes. We determined discharge at the gauging station for the 4 h after breaching on 26 October from the then-current station rating curve, which remained applicable until substantial aggradation began several hours after breaching. Because the stage-rating curve became invalid late on 26 October and because discharge was declining, we estimated hourly values of discharge by interpolation during the evening of 26 October (Appendix A and Table S1). We used estimated mean daily values of discharge at the gauge provided by the USGS (http://waterdata.usgs.gov/nwis) for the period 27 October 2011 through 4 February 2012 (the date of our last sediment concentration measurement).

Calculations of suspended-sediment flux over the range of time periods discussed relied on a mix of measured and estimated sediment concentrations. Incremental load calculations for the 4 h period following breaching were based on the sequence of measured sediment concentrations and corresponding discharge values determined from the stage-discharge rating. Longer-term estimates for 27 October 2011 through 4 February 2012 relied mostly on measured sediment concentration values, but suspended-sediment measurements were sparse for the period beginning with our last measurement on the afternoon of 26 October through 30 November 2011. For this period, we calculated suspended-sediment concentration on the basis of two power law regressions relating measured suspended-sediment concentration to time since breaching (Appendix A and Table S1). The first provided estimates for the period of rapidly changing concentration from late afternoon on 26 October to morning of 27 October. The second gave estimates of daily concentration from 27 October 2011 to 30 November 2011. Analysis using other regression models suggests that the estimated concentrations and resulting flux estimates for these periods have an uncertainty of about 30% (Appendix A and Table S1).

Our estimates of suspended-sediment flux passing the gauge likely underestimate the total sediment flux. The suspended-sediment total does not account for elevated, but unmeasured, sediment concentrations during an episode of high flow during 23–30 November, when peak flow exceeded 37 $m^3 s^{-1}$. Nor do the suspended-sediment measurements account for the bed load transport evident in the weeks following breaching, which we describe below.

4. Hydrologic and Geomorphic Response to Breaching

We present the upstream and downstream responses to breaching of Condit Dam at two time scales: (1) the first 5 h after breaching, which was the primary focus of our field efforts, and (2) the subsequent 15 week period of reservoir erosion and downstream channel response. Analysis at these two time scales allows us to link observed erosion processes and estimates of mass loss in the reservoir with downstream flow processes and sediment fluxes. It also permits analysis of the evolving relation between suspended-load and bed load fluxes.

4.1. Breach Day: 26 October 2011, 12:08 to 17:00

Rates and magnitudes of geomorphic response to breaching of Condit Dam were greatest on breach day. In addition, geomorphic processes eroding and transporting sediment downstream upon breaching of Condit Dam differed significantly from those following other dam removals.

4.1.1. At the Reservoir

Upon opening of the 5 m diameter outlet tunnel at the base of Condit Dam, Northwestern Lake drained rapidly (Figure 3). Observations at the reservoir show that most of the impounded water evacuated within 90 min; the reservoir water surface dropped 30 m during this time (Figure S2). During the first few minutes of post-breach drawdown, vegetated reservoir slopes previously affected by fluctuations of lake level as part of dam operations were exposed, but with little erosion evident. Beginning 11 min after breaching, however, the drawdown exposed unvegetated, saturated, fine-grained reservoir sediment on 30–55° side slopes near the dam and at the delta front. Exposure of this sediment triggered shallow-seated slope failures that progressed rapidly from the dam upstream through at least the lower 650 m of the reservoir. These failures fed large amounts of sediment into the incising reservoir channel and, in many cases, liquefied and evolved into slurries that flowed through the 5 m wide tunnel at the base of the dam (Animation S1). Slope failures also delivered hundreds to thousands of logs, relicts of a former sawmill on the banks of the reservoir, to the river (Animation S1 and Figure S1f). Within an hour of breaching, landsliding of the reservoir side slopes exposed pre-dam bedrock canyon walls. Also by this time, incision 120 m upstream of the dam exhumed a 4.5 m high timber-crib coffer dam used in original construction of the dam (Figures 2d and 3c). Analysis of imagery

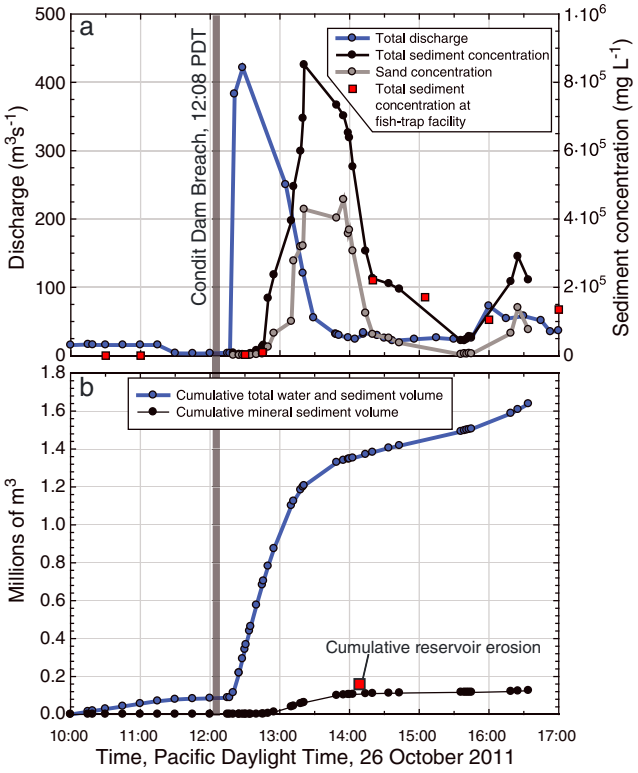

Figure 4. Time series of the first 5 h following breaching of Condit Dam of (a) discharge and sediment concentrations measured at sites 2.3 km (gauge) and 3 km (fish trap) downstream of the dam site; and (b) cumulative total volume discharge (sediment plus water volume) and estimated sediment volume discharge passing the gauging site 2.3 km downstream of the dam site, and estimated cumulative reservoir erosion as of 14:08 (red square). Vertical gray bar indicates time of breach. Source data provided in Table S1.

indicates that after 2 h, 160,000 m^3 of sediment had evacuated from the lower 650 m of the reservoir, about 10% of total reservoir sediment volume.

Although mass failures caused the majority of erosion in the lower reservoir, fluvial processes soon extended erosion upstream. At a river bend 650 m upstream of the dam (Figure 2c), a several-meter-high knickpoint formed 22 min after breaching. Here upstream propagation of reservoir erosion slowed as a knickzone spread laterally and carved into voluminous deposits forming the thickest part of the sedimentary delta (Figure 2d). Passage of the knickpoint from where it formed to upstream portions of the reservoir (Figure S3), through thickly accumulated sediment, resulted in steep, unstable side slopes that slid into the incising channel (Figure S4). Imagery indicates that substantial additional reservoir erosion occurred on the afternoon of breaching, beyond the 160,000 m^3 from the lower 650 m of the reservoir, extending to at least 1 km upstream of the dam by 17:00 on breach day.

4.1.2. Downstream

Downstream measurements showed rapid changes in discharge and sediment concentration, as well as relations between flow characteristics and resulting deposits (Figures 4 and 5). At the USGS gauge, flow was 3.1 $m^3 s^{-1}$ immediately prior to breaching, temporarily diminished from ~20 $m^3 s^{-1}$ base flow of the previous few days by intentional halting of reservoir outflow in preparation for breaching. The turbid and turbulent flood wave released by breaching arrived at the gauge at 12:17, 9 min after breaching (Animations S4 and S5), indicating a mean velocity of the flow front of 4.3 m s^{-1}. Flow stage increased for another 11 min, and flow reached a peak discharge of 421 $m^3 s^{-1}$ at 12:28 (Figures 4 and 5b), a discharge about equaling the 100 year recurrence interval flow. Flow declined swiftly, and by an hour later at 13:30 was about 55 $m^3 s^{-1}$ (Figure 4).

Sediment transport lagged the flood crest (Figure 4). From pre-breach sediment concentrations ranging between 5 and 15 mg L^{-1}, concentrations increased to about 3000 mg L^{-1} (0.1% by volume) at peak discharge. But as flow diminished, sediment concentrations increased rapidly, attaining 850,000 mg L^{-1} at 13:21, 53 min after peak discharge (and 72 min after breaching). Sediment concentrations subsequently diminished but remained mostly above 100,000 mg L^{-1} through our last measurements of the day at 16:34. Measurements at the fish trap site downstream show patterns in sediment concentration similar to those at the gauging station (Figure 4).

Measured fluxes of water and sediment passing the gauge during the first 5 h after breaching closely match measurements of water release and erosion from the reservoir. At 13:49, shortly after impounded water had visibly emptied from the reservoir, 101 min after breaching, and 92 min after arrival of the flow front at the gauge, 1.1 million m^3 of water and about 260,000 tonnes of suspended sediment had passed the gauging station. This is equivalent to 170,000 m^3 of reservoir sediment (for which measured bulk density

Figure 5. White Salmon River at USGS gauge site 2.3 km downstream of dam site, looking downstream: (a) 53 min before breaching; (b) 20 min after breaching, at discharge peak; (c) 76 min after breaching, at peak sediment concentration, with high water line evident; (d) ~2.5 h after breaching, discharge has returned to background and sediment concentration is falling; (e) 2 days after breaching, when channel has aggraded and migrating dunes indicate substantial sandy bed-material transport; and (f) 25 days after breaching, showing bar emergence.

was 1.5 tonnes m^{-3}), consistent with our estimate of 160,000 m^3 of sediment eroded from the lower 650 m of the reservoir in the first 2 h. By the time of our last breach-day sediment measurement at 16:34, a total of 1.4 million m^3 of water had passed the gauge along with 325,000 tonnes of sediment (equivalent to about 220,000 m^3 of reservoir sediment), about 12% of the total sediment impounded in the reservoir.

From these measurements at about the time of peak flow and during the ensuing phase of high-sediment-concentration flow, we can establish relations among sediment concentration, flow characteristics, and deposit sedimentology. Flow prior to breaching was clear and contained little sediment (Figures 4 and 5a). The flow front and subsequent rise to peak was turbulent, loud, and turbid but contained only about 3000 mg L^{-1} (0.1% by volume) at peak discharge. But as discharge decreased after the peak at 12:28, sediment concentration continued to increase, and by 13:10 was 400,000 mg L^{-1} (15% by volume). Despite

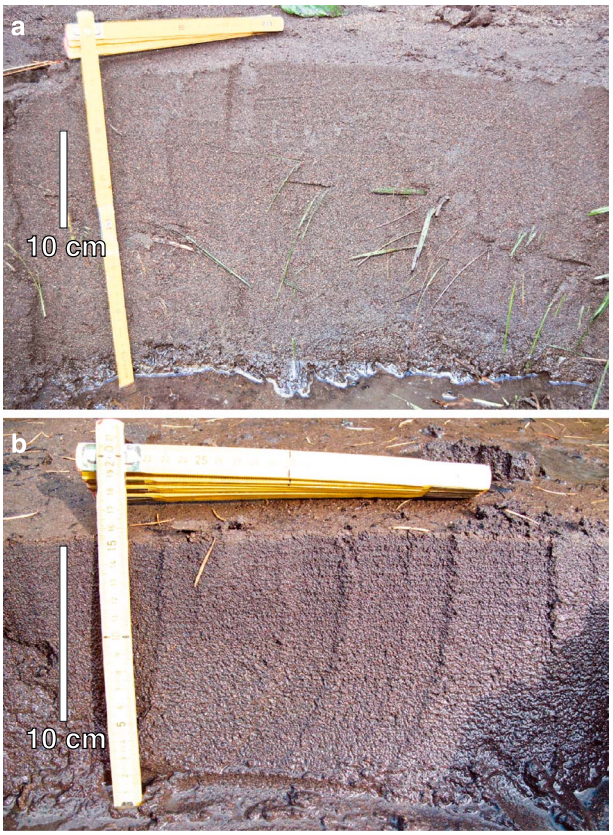

Figure 6. Photographs of deposits of 26 October 2011 Condit Dam breach. Segments in carpenter ruler about 22 cm long. (a) Grey hyperconcentrated flow deposit emplaced at about 13:10 (~1 h after breaching), when suspended sediment concentration was about 15% by volume. (b) Brown hyperconcentrated flow deposit emplaced about 13:20, when suspended sediment concentration was about 26% by volume and sand content of flow had approximately doubled. Grain-size distributions of samples from these deposits are shown in Figure 7.

this high-sediment concentration, flow remained loud and turbulent. Flow transformed markedly between 13:10 and 13:21 (Figure 5c), with both turbulence and sound substantially dampened. During this period, sediment concentration increased to 850,000 mg L^{-1} (32% by volume) and the relative sand content of the entrained sediment doubled to more than 50% (Figure 4). Flow at this time appeared viscous and placid, quietly rafting large coherent blocks of reservoir sediment along with abundant wood and organic debris (Figure 5c and Animations S4 and S5). Sediment concentration remained high, and flow remained smooth and quiet until about 14:00 when concentration dropped below 500,000 mg L^{-1} (20% by volume), after which turbulence and sound level increased.

In conjunction with these variations in flow character, two distinctive deposits were left at the gauge site and fish trap facility (Figure 6). Grey sand, up to 36 cm thick, was deposited locally along the valley margin (Figure A5). At the gauge site, the top of the deposit was at a stage height of 2.61 m. A thin extension of this sand deposit was locally traceable up to 50 cm higher (3.1 m stage height). A distinctly browner sand deposit, slightly lower and inset against the grey sand, was 10–20 cm thick with a top elevation at a stage height of 2.26 m at the gauge site. These deposits, which encased grassy vegetation in growth position, were preserved along the channel margin, away from and more than 3 m above the channel bed. Their position and encasement of vegetation indicate they were emplaced from settled suspended load. The higher grey sand deposit was inspected and sampled within 5 m of where we collected corresponding dip samples of the flow.

The grey deposit was composed chiefly of massively textured to faintly laminated, poorly sorted (1.1φ–1.9φ) [*Folk*, 1980] medium sand (Figure 6a). The deposit fined upward slightly, with the median grain size (d_{50}) ranging from about 0.4 mm at the base to 0.2 mm at the top. The correlative deposit at the fish trap facility had a similar composition with a d_{50} of about 0.2 to 0.3 mm. At all sites, the deposit was composed of approximately 80–90% sand (Figure 7 and Table S2).

The surface elevation of the grey sand indicates that it was deposited between about 13:00 and 13:10. At that time, flow stage was dropping after attaining a peak stage height of 3.71 m and sediment concentrations were rising quickly. But the flow was still loud and turbulent. At 13:10, when flow was at the elevation of the deposit surface, it had a sediment concentration of about 400,000 mg L^{-1} (15% sediment by volume). This sediment concentration is within the range of hyperconcentrated flow, and the massive to faintly stratified sand deposit is similar to deposits inferred to have been left by hyperconcentrated flows, primarily in conjunction with volcanic eruptions [e.g., *Pierson and Scott*, 1985; *Pierson*, 2005]. Sediment concentrations

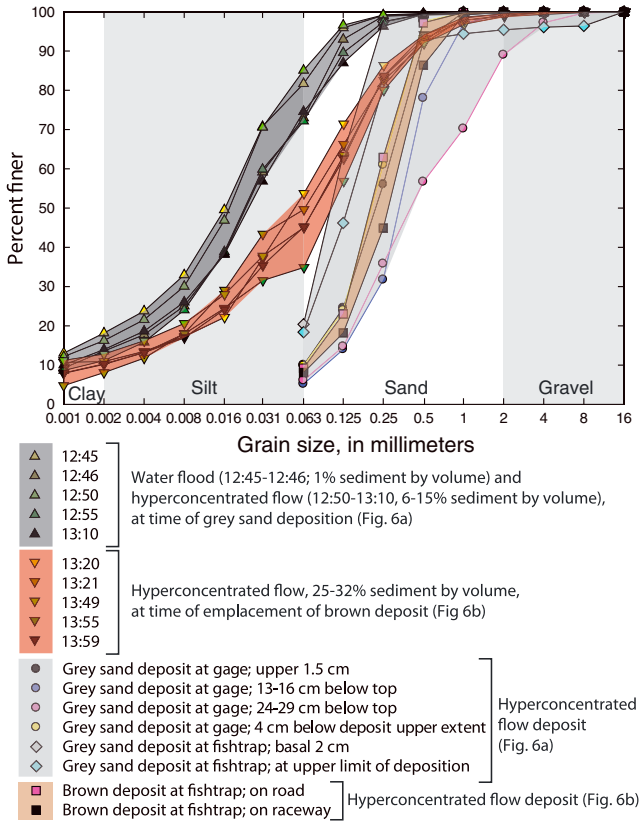

Figure 7. Grain-size distributions of suspended-sediment samples as flow reached hyperconcentrated phase (triangles, with sample time indicated) and associated deposits (shown in Figure 6) from 26 October 2011 Condit Dam breach. Complete particle size data are provided in Table S2.

defining hyperconcentrated flow vary but range mostly between 10 and 50% by volume. The lower bound is commonly defined by a sharp increase in the effectiveness of flow to suspend sand, which commonly occurs at volumetric sediment concentrations of about 5–10% [*Pierson*, 2005].

The deposit from the 13:00–13:10 phase of the hyperconcentrated flow is distinctly coarser than the suspended load of the corresponding flow, which ranged between 18 and 28% sand and 11 and 18% clay (by weight) between 12:45 and 13:10 (Figure 7). The difference between flow and deposit composition, in conjunction with the upward fining texture, indicates selective deposition of sand along the channel margin.

The lower brown deposit is also poorly sorted sand (sorting coefficient ~1.2φ), but it contained abundant organic detritus and had faint horizontal and planar laminae (Figure 6b). In contrast to the grey deposit, there is no size grading evident from top to bottom; samples (from the White Salmon fish trap facility) had d_{50} values of about 0.25 mm and total sand contents of 90% (Figure 7). The principal physical differences between the brown and grey deposits were the amount of organic content and the narrower sediment-size distribution and more evident lamination within the brown deposit (Figure 7).

The elevation of the brown deposit corresponds with the flow stage at about 13:20, when sediment concentration attained 700,000–850,000 mg L^{-1} (26–32% sediment by volume). Emplacement of the brown deposit was at the time of transition to more placid and viscous flow. Similar to the grey sand deposit, the coarser texture of the brown deposit relative to the corresponding flow composition (~50% sand, 40% silt, and 10% clay; Figure 7) indicates that it, too, was also formed in part by selective deposition.

Between 14:00 and 16:00, after the hyperconcentrated flow phase, flow stage stabilized and sediment concentration generally continued to drop. This period of stage stability was interrupted by a pulse of water having high sediment concentration between 16:00 and 16:30 (Figure 4), likely reflecting breakup of upstream log jams and/or continued mass movements of reservoir sediment. By our last measurements before leaving the site at 17:00, flow stage had dropped to 1.3 m, essentially equivalent to the 1.25 m stage height associated with the 20 m^3 s^{-1} flow passing the gauge prior to breaching. This close correspondence of flow stage in the hours before and after breaching indicates there was no or little net channel aggradation at the gauge site as a consequence of passage of the flood wave and subsequent pulse of high-sediment-concentration flow.

4.2. From 27 October 2011 to 4 February 2012

In the days and weeks after breaching of Condit Dam, the nature of erosion and transport processes evolved, and rates of erosion and downstream sediment transport slowed. Within the reservoir, erosion by mass movement gave way to fluvial erosion. Downstream, bed load transport became more evident and imparted greater change to channel morphology than did passage of the hyperconcentrated flow.

4.2.1. At the Reservoir

In the weeks after the 26 October 2011 breaching, reservoir erosion by knickpoint migration, channel incision, and small mass failures propagated upstream. After the immediate response on the afternoon of breaching, little change occurred in the lowermost 650 m of the reservoir because bedrock canyon walls were exposed and the old coffer dam prevented further incision until its removal in spring 2012 (Figure 2d). Farther upstream, however, erosion continued. Within 24 h of breaching, an estimated 200,000 m^3 of sediment had eroded from the reach extending 0.6 to 1.3 km upstream of the dam (Figure S4). Much of this erosion was instigated by a knickpoint that had propagated 2 km upstream of the dam (at an average rate of about 1 m/min; Figure S3). When added to our estimate of 160,000 m^3 of erosion in the lower 650 m of the reservoir, this indicates at least 360,000 m^3 of sediment eroded from the reservoir within 24 h of breaching. Available photography shows that most of this was during the afternoon of breaching. In the days following, erosion continued to extend upstream. Between 1.3 and 2 km upstream of the dam, time-lapse photos between 27 October and 1 November showed active incision, small mass failures that constricted the evolving channel, and exposure of bedrock (Figure S6). By 2 November (1 week after breaching), this reach had also lost about 200,000 m^3 of sediment. From these observations and our estimates of reservoir erosion in the lower 1.3 km in the 24 h after breaching, we estimate at least 550,000 m^3 of sediment was eroded from the lower 2 km of the reservoir by 2 November, a week after breaching. Additional reservoir sediment eroded during this time from farther upstream and from tributary channels, but our photography coverage is not adequate to estimate the timing and volume of that erosion.

Within 1 to 2 weeks of breaching, reservoir erosion slowed substantially. The knickpoint continued to migrate upstream at a diminishing rate (~0.05 m/min), reaching a bridge near the head of the reservoir (2.6 km upstream) within 8 days of breaching. Within 2 weeks, the knickpoint had extended to about 2.9 km upstream of the dam, about 200 m beyond the pre-breach estimate of the upstream extent of reservoir sediment [*Washington State Department of Ecology*, 2007]. By this time, erosion was concentrated in the upper reservoir, 2–2.9 km upstream of the dam, and in tributaries that entered the former reservoir.

Differencing of the pre-breach and 21 December 2011 post-breach DEMs indicates a minimum of 1.1 million m^3 had eroded from the reservoir as of 8 weeks (56 days) following breaching [*Riverbend Engineering and JR Merit*, 2012] (Figure 8a). This eroded volume, approximately half of which evacuated in the week after breaching, was about 60% of the total volume of impounded sediment as estimated in 2006. A subsequent lidar survey in July 2012 [*Riverbend Engineering and JR Merit*, 2012] showing 1.3 million m^3 of total erosion indicates reservoir erosion slowed substantially after 21 December 2011.

4.2.2. Downstream

Measurements at the gauge site and fish trap facility showed that sediment concentration declined significantly in the days and weeks after breaching (Figure 8b). By the day after breaching, sediment concentration had decreased to about 50,000 mg L^{-1}. Owing to channel aggradation and consequent difficulties with maintaining clear pump-sampler intakes, sediment concentrations measured from pump samples are highly variable for the 2 weeks after breaching. These difficulties also resulted in few samples between 2 November and 1 December. However, limited dip samples and depth-integrated cross-section measurements at the gauge site between 2 and 8 November show sediment concentrations between 10,000 and 25,000 mg L^{-1}. By 1 December, resumed pump samples show sediment concentration had declined to less than 500 mg L^{-1}, although concentrations rose during periods of high flow (Figure 8c). During this post-breach period, the sand content of the suspended load remained high—generally over 30% and briefly attaining 90% during episodes of high concentration.

Sediment transport measurements (and estimates) at the gauging station accord with erosion estimates at the reservoir. By 13:06 on 27 October, 25 h after breaching, approximately 615,000 tonnes of suspended sediment had passed the gauging station, equivalent to about 410,000 m^3 of eroded reservoir sediment. This estimate exceeds, but is consistent with, the minimum of 360,000 m^3 of reservoir sediment estimated to have vacated the lower 1.3 km of reservoir within 24 h of breaching. By 2 November, we estimate 1 million tonnes of suspended load had passed the gauge, equivalent to 680,000 m^3 of eroded reservoir sediment, also slightly exceeding our estimate of a minimum of 550,000 m^3 eroded from the lower 2.0 km of the reservoir by that time. The 21 December 2011 lidar survey indicated a minimum of 1.1 million m^3 of total reservoir

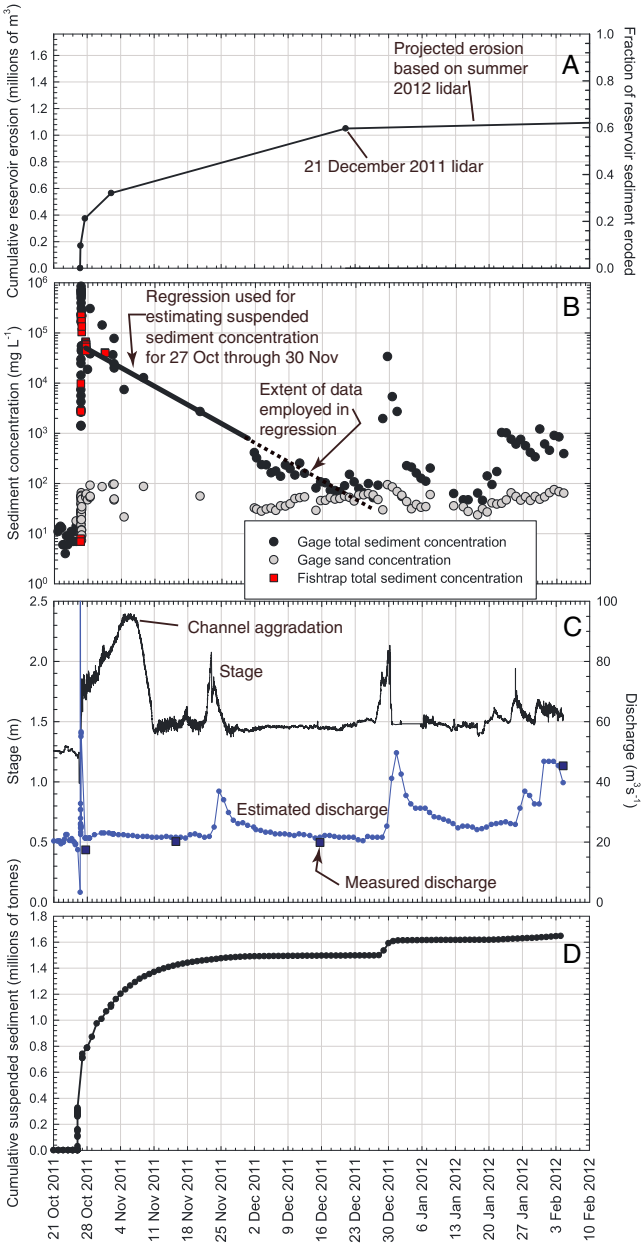

Figure 8. Time series, from 21 October 2011 to 4 February 2012, of (a) cumulative reservoir erosion (and fraction of total reservoir sediment eroded), (b) downstream suspended sediment concentration at two sites (gauge 2.3 km downstream of dam; fish trap 3.0 km downstream), (c) stage and discharge (at gauge), and (d) cumulative suspended-sediment flux at gauge site. Gradual stage rise and fall (Figure 8c) from ~27 October to 9 November illustrates bed aggradation and passage of bed material sediment wave. Source data provided in Table S1.

erosion, about 20% greater than our estimate of 935,000 m^3 (1.4 million tonnes) of suspended sediment passing the gauge site. At the time of our last measurement on 4 February 2012, we estimate that a minimum of 1.5 million tonnes of suspended load had passed the gauging station, equivalent to 1 million m^3 of eroded reservoir sediment—55% of the total volume of impounded sediment. That estimate is about 25% less than the 1.3 million m^3 of reservoir erosion determined from the July 2012 lidar survey [*Riverbend Engineering and JR Merit*, 2012].

The estimates of reservoir erosion and suspended-sediment flux show that suspended-sediment transport at the gauging station accounted for nearly all of the sediment transported from the reservoir during the first week after breaching. About 40% of the suspended sediment passing the gauge during the first week passed during the 4 h of high-concentration flow between 13:00 and 17:00 on the day of the breach. Discrepancies described above between estimates of suspended-sediment flux and lidar-based measurements of reservoir erosion in the months following breaching are within the range of uncertainty of the measurements, but they are also consistent with bed load transport—which is not included in our sediment transport measurements and flux estimates at the gauging station—becoming a more important process in moving sediment downstream in the days, weeks, and months following breaching.

4.3. Bed Aggradation and Bed Load Transport

Although the majority of sediment exiting the reservoir was transported downstream as suspended load, bed load transport was substantial and had significant effects on the channel downstream of the dam. A rising flow stage under declining discharge at the gauging station by 20:00 on breach day (26 October) indicates the onset of bed aggradation (Figure 8c). This aggradation coincided with substantial sand transport by dunes [*Simons et al.*, 1965] migrating down a widening and shoaling channel. We observed these dunes on 27–28 October (Figure 5e) and their passage is also recorded by high-frequency oscillations of stage measurements in the week after breaching as the

channel bed aggraded (Figure 8c). Maximum channel aggradation reached a stage height of 2.4 m, more than a meter higher than the stage height for an equivalent discharge prior to breaching. When aggradation culminated on about 7 November, the river was transporting gravel, inferred from gravel preserved on and just below the fill surface after subsequent incision (Figure S5). Substantial gravel transport may have corresponded with reduced bed-stage oscillations beginning about 1 November, when flow stage reached about 2.1 m (Figure 8c).

After the channel attained its maximum aggradation level in early November, the river incised through the fill. By 10 November, the river had incised nearly 1 m and attained a stable stage of about 1.5 m (Figure 8c), about 0.2 m higher than low-flow stage before dam breaching. Bed conditions, however, had changed markedly from pre-breach conditions. Pools had filled with gravel, and sand-and-gravel bars flanked the channel. High-frequency stage oscillations between 11 and 21 November (Figure 8c) may indicate return to bed load transport of mostly sand and passage of low-amplitude dunes.

5. Discussion

The Condit Dam removal was unique in the combination of its size, rapid breaching, large sediment volume, and fine-grained composition of the impounded sediment. These combined factors resulted in a geomorphic response that had elements common to many past removals. Some aspects of the response, however, such as the prevalent mass movements in the reservoir and the downstream hyperconcentrated flow, were unusual and give new insights on potential magnitudes, rates, and processes by which dam decommissionings potentially affect river corridors. The rapid removal of this tall constructed dam also gives insight on geomorphic responses to breachings of natural dams and other disturbances that inject substantial sediment volumes into rivers.

Dam removal by rapid breaching of a reservoir impounding a large volume of fine-grained sediment, as at Condit, typically is not intentional and is unlikely to be common because of the rapid and profound response, both upstream and downstream. In the case of Condit Dam, rapid dewatering led to extensive mass movements of reservoir sediment and rapid incision of the developing channel. These mass movements conveyed sediment to the channel at rates and magnitudes that exceeded what would have been possible by only fluvial incision and widening. Consequently, the Condit removal had a very high percentage—about 20%—of its reservoir sediment evacuated within 24 h of breaching, the period when mass movements were most active. By comparison, the breaching of Marmot Dam, 15 m tall with an impoundment totally filled with sand and gravel, triggered erosion of only about 15% of its impounded sediment in the 2 weeks following rapid breaching, despite the reservoir sediment being narrowly confined and coarse grained [*Major et al.*, 2012]. The differences in responses owe mostly to the reservoir behind Marmot Dam being devoid of a deep pool (hence no rapid dewatering) and eroding mainly by relatively slower fluvial processes of knickpoint retreat, channel incision, and channel widening. At Condit Dam, fluvial processes became the primary agent of erosion only after the size and frequency of mass movements diminished as the wave of channel incision moved upstream into and through the thickest accumulation of sandy sediment.

Another critical aspect was the fine-grained composition of the reservoir sediment. The sediment behind Condit Dam was 95% sand, silt, and clay. Although impoundments behind other dams had similar sediment compositions, including the impoundments behind the now-removed Elwha River dams, few large dams impounding such fine-grained sediment have been removed (Table 1). The fine texture and resulting low permeability likely contributed to the prevalence of mass movements in the reservoir by promoting non-equilibrium pore-water pressure in the sediment as the reservoir was drawn down very rapidly, thereby reducing effective stress, creating adverse seepage forces, and disrupting soil structure [e.g., *Morgenstern*, 1963]. Generation of non-equilibrium pore-water pressure also likely contributed to rapid mobilization into slurries of some mass failures [e.g., *Iverson*, 2014].

Rapid introduction of fine-grained sediment by mass movements of reservoir sediment to the channel profoundly affected downstream flow conditions. Drawdown of the reservoir promoted the most intense period of mass movement just as water flow out of the reservoir was diminishing. This led to flow attaining exceptional sediment concentrations in the 3 h after breaching, up to 850,000 mg L^{-1} (32% by volume). As sediment concentration increased, flow became hyperconcentrated, at first noisy and turbulent but then quiet and viscous. This transformation corresponded closely with sediment concentration exceeding about

500,000 mg L^{-1} and a marked increase in suspended sand content (Figure 4a). The period of hyperconcentrated flow, which lasted about 2 h, conveyed about 10% of the total volume of impounded reservoir sediment down the channel. The hyperconcentrated flow also moved a large amount of sandy sediment several kilometers, through the downstream bedrock gorge, very rapidly.

We are unaware of any previous dam removal producing hyperconcentrated flow. For future removals hyperconcentrated flow like this may be a possible outcome for fine-grained reservoirs breached rapidly, especially where deposits are thick and impoundments deep. Moreover, sediment-laden flows, such as documented here, and more highly sediment-laden debris flows are commonly associated with rapid natural introduction of large sediment volumes into fluvial systems. These sediment pulses can occur during volcanic eruptions [*Pierson and Scott*, 1985; *Cronin et al*., 1999; *Pierson*, 2005], by landslides [e.g., *Guthrie et al*., 2012; *Iverson*, 2014], or when floods entrain great volumes of channel sediment such as during outburst floods resulting from failures of natural dams [*O'Connor et al*., 2001; *Procter et al*., 2010; *Carrivick*, 2011].

Our tightly constrained observations and measurements clarify relations between character and concentration of hyperconcentrated flow and resulting deposits. Both the strongly turbulent and dampened phases of hyperconcentrated flow left distinctive sand deposits at the channel margin (Figures 6 and 7). Both deposits had coarser grain-size compositions than did the flow at the time of emplacement, indicating that the deposits formed by selective deposition rather than en masse emplacement. However, the brown deposit associated with the less turbulent, more viscous flow phase was slightly less differentiated from the sediment of its source flow (Figure 7). Although such flows and their deposits are likely to be uncommon with dam decommissionings, their interpretation is important for hazard and paleoenvironmental assessments in other settings [*Pierson*, 2005].

As observed following other dam removals, coarse bed material transport at Condit Dam lagged behind downstream transport of finer sediment. It was several hours after the extraordinary pulse of suspended load exited the reservoir before substantial bed load transport became evident at the gauging station 2.3 km downstream, as suggested by channel aggradation beginning 8 h after breaching and observations of migrating dunes the following day. Substantial gravel transport past the gauging station probably did not begin until nearly a week after breaching, and when aggradation culminated 10–12 days after breaching, abundant gravel was transported as bed load, capping the soon-to-be-incised fill.

Suspended-sediment transport followed first by sandy bed load and then by gravel was also observed following the breaching of Marmot Dam. There, silt and sand swept downstream first as suspended load, but within a few hours of breaching, substantial sand-dominated bed load transport began passing a measurement station ~400 m downstream of the dam site. Significant gravel transport began about 18–20 h after breaching, and as at Condit Dam, it also coincided with rapid bed aggradation [*Major et al*., 2012].

The leading edge of gravel released from breaching of Condit and Marmot dams moved downstream at similar rates. Below Marmot Dam, gravel moved downstream on the Sandy River at a rate of approximately 20 m h^{-1}. Below Condit Dam, gravel capping the peak of the aggradational fill observed at the gauge site indicates a minimum transport rate of 16 m h^{-1}. Despite the different styles and rates of fine-grained sediment transport resulting from these two dam removals, similarities in gravel transport conditions likely owe to similar gravel transport processes and rates associated with steep, confined valleys under conditions of abruptly increased, mixed-size bed load [e.g., *Wilcock et al*., 2001; *Wilcock and Crowe*, 2003].

The fate of downstream aggradation following breaching of Condit and Marmot dams differed, however. At both sites, downstream aggradation was rapid, most in the few days or weeks following breaching. At Condit, however, the sand and gravel fill were soon reincised; the channel lowered to near its original elevation at the gauge site within 15 days of breaching. This rapid reincision reflected both the sparse gravel in the channel fill and the diminishment of sediment supply from the reservoir. In contrast, at Marmot, the sand and gravel fill persisted for at least 7 years after breaching. Incision at Marmot has been slower, in part, because sand and gravel continued to be slowly supplied from the reservoir reach and because of coarse armoring of the aggraded channel bed [*Major et al*., 2012]. These differences highlight

the influence of the composition of reservoir sediments and downstream deposits on the rate and magnitude of post-breaching channel responses.

Although the decommissioning of Condit Dam was unique and not likely to be a close analog for many intentional dam decommissionings, some aspects of the response we have described here clarify the range of possible processes and outcomes associated with dam removal. In particular, the Condit Dam decommissioning shows the importance of the types of processes evacuating reservoir sediment in controlling the overall response. An ability to better define the conditions associated with reservoir-erosion-process regimes would enable better prediction (and modeling) of the outcomes of different strategies. Downstream channel responses associated with bed load transport are broadly predictable with sediment transport models [e.g., *Cui*, 2007; *Cui and Wilcox*, 2008]. As is evident in the disparate channel responses at Marmot and Condit, the success of such models will depend critically on accurate assessments of the volume and composition of the reservoir sediment likely to enter the channel.

6. Conclusions

The breaching of Condit Dam provided an opportunity to monitor the effects of decommissioning a tall (38 m) dam impounding a substantial volume (1.8 million m^3) of fine-grained sediment (mostly sand, silt, and clay). Unlike most other decommissioned tall dams impounding voluminous fine-grained sediment, this dam was breached rapidly and the full base-level change was imposed on a time scale of minutes rather than months or years. The unusual decommissioning led to the following outcomes, many unique to large-dam removals observed so far:

1. Rapid drawdown of the reservoir pool led to rapid channel incision and mass movements of reservoir sediment.
2. Mass movements, partly facilitated by the fine-grained sediment composition, delivered sediment to the channel faster than would fluvial processes such as knickpoint migration and channel incision and extension.
3. Mass movements contributed to substantial and rapid removal of reservoir sediment. Within 2 h of breaching, about 10% of the impounded sediment was removed, and within 24 h, about 20% was removed.
4. Several mass movements to the channel rapidly mobilized into slurries that resulted in downstream hyperconcentrated flow in the few hours after breaching. This flow attained sediment concentrations as great as 850,000 mg L^{-1} (32% sediment by volume). Such flow concentrations, not previously documented for dam removals, are nevertheless common when channels are overloaded by sediment from landslides, natural dam failures, and volcanic eruptions.
5. Channel margin deposits left by the hyperconcentrated flow are similar to previously documented deposits left by such flows, but our concurrent measurements of flow composition show that in this case they were formed mainly by selective deposition of sand from suspension.
6. Most of the eroded reservoir sediment passed downstream as suspended load. Substantial sand and gravel bed load transport followed after several hours. Bed material transport and deposition aggraded the channel 1–2 m at our measurement site 2.3 km downstream from Condit Dam during the 10 days following breaching. This fill was incised completely 5 days later as a consequence of diminished sediment supply exiting the reservoir and sparse gravel composition, which inhibited armoring of the channel fill during incision.

These overall observations and interpretations, although associated with an uncommon style of dam removal, nevertheless, give insights that may be useful for predicting the consequences of future dam removals. A key conclusion is that the processes that erode sediment from the reservoir exert strong control on the rate of erosion and consequent downstream transport of sediment. From this study, it is evident that controls on these processes include dam height, the rate of breaching, and composition of the impounded sediment. The composition of the impounded sediment influences downstream flow conditions and sediment transport processes and also affects longer-term channel response. In particular, these findings support continued efforts to predict and model responses to dam removals by clarifying the types and possible effects of processes entraining, moving, and depositing sediment in newly reconnected rivers.

Appendix A

Owing to periods of missing data, we augmented measured sediment concentration with estimates of sediment concentration in order to compute suspended-sediment flux in the immediate aftermath of breaching, and daily sediment flux for the subsequent 15 weeks. Estimates of concentration were based on regression models that related concentration to time since breaching for two different time periods. The regression for rapidly changing concentration between our last measurement at 16:34 on 26 October and our first measurement at 12:47 on 27 October was derived from five sediment concentration measurements (our last two on 26 October and first three on 27 October), a time when both concentration and flow discharge were declining. A power law regression provided the best fit to the data. We also explored a multiparameter linear regression model that related concentration to both discharge and time since breaching. Exploration of these regression models indicates uncertainty in our estimates of suspended-sediment concentration during this period of rapid change of as much as 30%. Because of channel aggradation, the discharge-stage rating was no longer valid late on 26 October. Consequently, we estimated discharge for the period between 17:00 and 24:00 on 26 October by interpolation between 56 $m^3 s^{-1}$ (the discharge at our last measurement on 26 October) and 21.2 $m^3 s^{-1}$ (the estimated mean daily discharge on 27 October).

Daily suspended-sediment transport totals from 27 October to 30 November 2011 were based on regression analysis of concentration, whereas transport from 1 December 2011 to 4 February 2012 was based on daily concentration measurements. The regression used to estimate daily concentrations from 27 October to 30 November was derived from 41 sediment concentration measurements between 27 October and 27 December, a period in which concentration declined but associated flow (flow at times of suspended-sediment concentration measurements) varied only between 21.2 and 24.9 $m^3 s^{-1}$. For the 7 days of missing sediment concentration measurements during the period 1 December 2011 to 4 February 2012, we estimated concentration values by averaging measurements of previous and subsequent days. Complete records and calculations are provided in Table S1.

We used estimates of mineral grain density and bulk sediment density to convert measurements and estimates of concentration and mass flux to sediment volumes and volume flux. To determine the volumetric percentage of sediment in transport, we converted measured sediment concentrations (in mg L^{-1}) using a grain density of 2.6 tonnes m^{-3}. To relate suspended-sediment flux at the gauging station to volumetric measurements of reservoir erosion, we converted mass flux measured at the gauging station to an equivalent erosion volume using a factor of 1.5 tonnes m^{-3}, a density we measured from a large coherent block of reservoir sediment entrained in and rafted downstream by the hyperconcentrated flow.

Acknowledgments

Wilcox's participation in this work was supported by the National Science Foundation (EAR-0922296, EPS-1101342). We thank Erika Colaiacomo for her many contributions to this work. We also thank Andy Maser, Steve Stampfli, Joshua Epstein, and Dennis Gathard for photos; Larry Moran (JR Merit) for aerial video; and Tom Hickey and Todd Olson (PacifiCorp), Peter Stroud (Kleinfelder), and Chris Pitcher (Riverbend) for access and data sharing. Robert Livesay, Elena Evans, Tom Pierson, and Chauncey Anderson provided field assistance. Flow and sediment measurements at the USGS gauging station and fish trap facility were conducted by Heather Bragg, Dale Melton, Adam Mosbrucker, Dave Piatt, Kurt Spicer, and Mark Uhrich. Jim Parham assisted with providing gauging station data. Adam Mosbrucker and Matt Logan helped compile some of the auxiliary video files. Reviews by Chuck Podolak, Matt Collins, Jim Pizzuto, Gordon Grant, and Associate Editor John Buffington improved the manuscript. Any use of trade, firm, or product names is for descriptive purposes only and does not imply endorsement by the authors, funding agencies, or U.S. Government.

References

Ambers, R. K. (2001), Using the sediment record in a western Oregon flood-control reservoir to assess the influence of storm history and logging on sediment yield, *J. Hydrol.*, *244*(3), 181–200.

American Rivers (2013), 62 Dams removed to restore rivers in 2012. [Available at http://www.americanrivers.org/newsroom/press-releases/2013/62-dams-removed-in-2012.html, Accessed 3 July 2013.]

Bountry, J. A., Y. G. Lai, and T. J. Randle (2013), Sediment impacts from Savage Rapids Dam removal, Rogue River, Oregon, in *The Challenges of Dam Removal and River Restoration*, *Geol. Soc. Am.*, edited by J. V. DeGraff and J. E. Evans, pp. 93–104, Boulder, Colo.

Cannatelli, K. M., and J. C. Curran (2012), Importance of hydrology on channel evolution following dam removal: Case study and conceptual model, *J. Hydraul. Eng.-ASCE*, *138*(5), 377–390, doi:10.1061/(asce)hy.1943-7900.0000526.

Carrivick, J. L. (2011), Jökulhlaups: Geological importance, deglacial association and hazard management, *Geol. Today*, *27*(4), 133–140.

Collins, M. L., et al. (2013), Physical and biological responses to dam removal sediment release, Patapso River, Maryland, *EOS Trans. AGU*, Fall Meet. Suppl., Abstract EP43A-0821.

Cronin, S. J., V. Neall, J. Lecointre, and A. Palmer (1999), Dynamic interactions between lahars and stream flow: A case study from Ruapehu volcano, New Zealand, *Geol. Soc. Am. Bull.*, *111*(1), 28–38.

Cui, Y. (2007), Examining the dynamics of grain size distributions of gravel/sand deposits in the Sandy River, Oregon with a numerical model, *River Res. Appl.*, *23*(7), 732–751, doi:10.1002/rra.1012.

Cui, Y., and A. Wilcox (2008), Development and application of numerical models of sediment transport associated with dam removal, in *Sedimentation Engineering: Theory, Measurements, Modeling, and Practice, ASCE Manual 110*, edited by M. H. Garcia, chap. 23, pp. 995–1020, ASCE, Reston, Va.

Czuba, C. R., T. J. Randle, J. A. Bountry, C. S. Magirl, J. A. Czuba, C. A. Curran, and C. P. Konrad (2011a), Anticipated sediment delivery to the lower Elwha River during and following dam removal, in *Coastal Habitats of the Elwha River, Washington—Biological and Physical Patterns and Processes Prior to Dam Removal, U.S. Geol. Surv.*, edited by J. J. Duda, J. A. Warrick, and C. S. Magirl, pp. 27–46, Reston, Va.

Czuba, J. A., C. S. Magirl, C. R. Czuba, E. E. Grossman, C. A. Curran, A. S. Gendaszek, and R. S. Dinacola (2011b), Sediment load from major rivers into Puget Sound and its adjacent waters, 4 pp., U.S. Geol. Surv., Fact Sheet 2011-3083.

DeGraff, J. V., and J. E. Evans (Eds.) (2013), *The Challenges of Dam Removal and River Restoration*, GSA Reviews in Engineering Geology, vol. 21, Geol. Soc. Am., Boulder, Colo.

Downs, P. W., Y. Cui, J. K. Wooster, S. R. Dusterhoff, D. B. Booth, W. E. Dietrich, and L. S. Sklar (2009), Managing reservoir sediment release in dam removal projects: An approach informed by physical and numerical modelling of non-cohesive sediment, *Int. J. River Basin Manage.*, *7*(4), 433–452, doi:10.1080/15715124.2009.9635401.

Doyle, M. W., E. H. Stanley, and J. M. Harbor (2003a), Channel adjustments following two dam removals in Wisconsin, *Water Resour. Res.*, *39*(1), 1011, doi:10.1029/2002WR001714.

Doyle, M. W., E. H. Stanley, J. M. Harbor, and G. G. Grant (2003b), Dam removal in the United States: Emerging needs for science and policy, *Eos Trans. AGU*, *84*(4), 29–36, doi:10.1029/2003EO040001.

Draut, A. E., and A. C. Ritchie (2013), Sedimentology of new fluvial deposits on the Elwha River, Washington, USA, formed during large-scale dam removal, *River Res. Appl.*, doi:10.1002/rra.

Duda, J. J., J. A. Warrick, and C. S. Magirl (Eds.) (2011), Coastal habitats of the Elwha River, Washington—Biological and physical patterns and processes prior to dam removal, 264 pp., U.S. Geol. Surv. Sci. Invest. Rep., 2011-5120.

Evans, E., and A. C. Wilcox (2013), Fine sediment infiltration dynamics in a gravel-bed river following a sediment pulse, *River Res. Appl.*, doi:10.1002/rra.2647.

Federal Energy Regulatory Commission (2002), Final supplemental final environmental impact statement, Condit Hydroelectric Project Washington FERC No. 2342, Washington, D. C.

Finley Engineering (2006), Condit Dam and Northwestern Lake hydrographic surveys final report, Prepared for PacifiCorp, Portland, Oreg.

Folk, R. L. (1980), *Petrology of Sedimentary Rocks*, 182 pp., Hemphill Publishing Company, Austin, Tex.

G&G Associates (2004), Condit hydroelectric project removal, sediment behavior analysis report, Prepared for PacifiCorp, Portland, Oreg.

Graf, W. L. (Ed.) (2002), *Dam Removal Research: Status and Prospects*, 151 pp., H. John Heinz III Center for Science, Economics and the Environment, Washington, D. C.

Gray, J. R., and F. J. M. Simoes (2008), Estimating sediment discharge, in *Sedimentation Engineering*, edited by M. H. Garcia, pp. 1067–1088, American Society of Civil Engineering Manuals and Reports on Engineering Practice, Reston, Va.

Guthrie, R., P. Friele, K. Allstadt, N. Roberts, S. Evans, K. Delaney, D. Roche, J. Clague, and M. Jakob (2012), The 6 August 2010 Mount Meager rock slide-debris flow, Coast Mountains, British Columbia: Characteristics, dynamics, and implications for hazard and risk assessment, *Nat. Hazards Earth Syst. Sci.*, *12*(5), 1277–1294.

Iverson, R. M. (2014), Debris flows: Behaviour and hazard assessment, *Geol. Today*, *30*, 15–20.

Kibler, K., D. Tullos, and M. Kondolf (2011), Evolving expectations of dam removal outcomes: Downstream geomorphic effects following removal of a small, gravel-filled dam, *JAWRA J. Am. Water Resour. Assoc.*, *47*(2), 408–423, doi:10.1111/j.1752-1688.2011.00523.x.

Kleinfelder (2007), Sediment sampling and analysis report, Northwestern Lake, Condit Hydroelectric Project, Prepared for PacifiCorp Energy, Beaverton, Oreg.

Magirl, C. S., P. J. Connolly, B. Coffin, J. J. Duda, C. A. Curran, and A. E. Draut (2010), Sediment management strategies associated with dam removal in the State of Washington, paper presented at Proceedings of the 2nd Joint Federal Interagency Conference, Las Vegas, Nev., 28 June–July 1.

Major, J. J., K. R. Spicer, and R. A. Collins (2010), Time-lapse imagery of the breaching of Marmot Dam, Oregon, and subsequent erosion of sediment by the Sandy River—October 2007 to May 2008, 5 pp., U.S. Geol. Surv. Data Ser., 521.

Major, J. J., et al. (2012), Geomorphic response of the Sandy River, Oregon, to removal of Marmot Dam, *USGS Prof. Pap.*, *1792*, 64.

Mead & Hunt, Kleinfelder, and JR Merit (2011), Project removal design report, Condit Hydroelectric Project Decommissioning FERC Project No. 2342, Prepared for PacifiCorp Energy.

Morgenstern, N. R. (1963), Stability charts for earth slopes during rapid drawdown, *Geotechnique*, *13*, 121–131.

O'Connor, J. E., J. H. I. Hardison, and J. E. Costa (2001), Debris flows from failures of Neoglacial-age moraine dams in the Three Sisters and Mt. Jefferson Wilderness areas, Oregon, *U.S. Geol. Surv. Prof. Pap.*, *1606*, 93.

Pearson, A. J., N. P. Snyder, and M. J. Collins (2011), Rates and processes of channel response to dam removal with a sand-filled impoundment, *Water Resour. Res.*, *47*, W08504, doi:10.1029/2010WR009733.

Pierson, T. C. (2005), Hyperconcentrated flow—Transitional process between water flow and debris flow, in *Debris-Flow Hazards and Related Phenomena*, edited by M. Jakob and O. Hungr, pp. 159–202, Springer-Praxis, Berlin Heidelberg.

Pierson, T. C., and K. M. Scott (1985), Downstream dilution of a lahar: Transition from debris flow to hyperconcentrated streamflow, *Water Resour. Res.*, *21*, 1511–1524, doi:10.1029/WR021i010p01511.

Pizzuto, J. (2002), Effects of dam removal on river form and process, *BioScience*, *52*(8), 683–691.

Procter, J., S. J. Cronin, I. C. Fuller, G. Lube, and V. Manville (2010), Quantifying the geomorphic impacts of a lake-breakout lahar, Mount Ruapehu, New Zealand, *Geology*, *38*(1), 67–70.

Randle, T. J., and B. Greimann (2004), Sediment impact analysis for the proposed Hemlock Dam removal project: Gifford Pinchot National Forest, Skamania County, 63 pp., U.S. Bureau of Reclamation Technical Service Report, Denver, Colo.

Riverbend Engineering, and JR Merit (2012), Annual sediment assessment report-2012, Condit Hydroelectric Project Decommissioning FERC Project No. 2342, Prepared for PacifiCorp Energy.

Roering, J. J., J. Marshall, A. M. Booth, M. Mort, and Q. Jin (2010), Evidence for biotic controls on topography and soil production, *Earth Planet. Sci. Lett.*, *298*(1), 183–190.

Sawaske, S. R., and D. L. Freyberg (2012), A comparison of past small dam removals in highly sediment-impacted systems in the U.S, *Geomorphology*, *151–152*(0), 50-58.

Service, R. F. (2011), Will busting dams boost salmon?, *Science*, *334*(6058), 888–892.

Simons, D. B., E. V. Richardson, and C. F. J. Nordin (1965), Sedimentary structures generated by flow in alluvial channels, in *Primary Sedimentary Structures and Their Hydrodynamic Interpretation*, *Society of Economic Paleontologists and Mineralogists Special Publication*, vol. 12, edited by G. V. Middleton, pp. 34–52, SEPM, Fort Collins, Colo.

Tullos, D., and H.-W. Wang (2014), Morphological responses and sediment processes following a typhoon-induced dam failure Dahan River, Taiwan, *Earth Surf. Processes Landforms*, *39*, 245–258, doi:10.1002/esp.3446.

USEPA (2004), Milltown Reservoir sediments operable unit of the Milltown Reservoir/Clark Fork River superfund site record of decision, U.S. Environmental Protection Agency Region 8, Helena, Mont.

Walter, C., and D. D. Tullos (2010), Downstream channel changes after a small dam removal: Using aerial photos and measurement error for context; Calapooia River, Oregon, *River Res. Appl.*, *26*(10), 1220–1245, doi:10.1002/rra.1323.

Warrick, J. A., J. J. Duda, C. S. Magirl, and C. A. Curran (2012), River turbidity and sediment loads during dam removal, *Eos Trans. AGU*, *93*(43), 425–426, doi:10.1029/2012EO430002.

Washington State Department of Ecology (2007), Condit Dam Removal Final SEPA Supplemental Environmental Impact Statement (FSEIS), Yakima, Wash.

Watershed Sciences Inc. (2012), Condit Dam, Washington LiDAR data, Corvallis, Oreg.
Wilcock, P. R., and J. C. Crowe (2003), Surface-based transport model for mixed-size sediment, *J. Hydraul. Eng.-ASCE*, *129*(2), 120–128, doi:10.1061/(asce)0733-9429(2003)129:2(120).
Wilcock, P. R., S. T. Kenworthy, and J. C. Crowe (2001), Experimental study of the transport of mixed sand and gravel, *Water Resour. Res.*, *37*, 3349–3358, doi:10.1029/2001WR000683.
Wilcox, A. C. (2010), Sediment transport and deposition resulting from a dam-removal sediment pulse: Milltown Dam, Clark Fork River, MT, *EOS Trans. AGU*, Fall Meet. Suppl., Abstract H31E-1045.
Wildman, L. A. S., and J. G. MacBroom (2005), The evolution of gravel bed channels after dam removal: Case study of the Anaconda and Union City Dam removals, *Geomorphology*, *71*(1-2), 245–262, doi:10.1016/j.geomorph.2004.08.018.